

## Microtribological Properties of DLC Films Prepared by Different Methods

Xin Li<sup>\*</sup>, Hongping Zhu and Hui Miao

School of Information Science and Engineering, Shenyang University of Technology, Shenyang 110870, China

Received 3 April 2018; Accepted 29 June 2018

### Abstract

Diamond-like-carbon (DLC) films are considered ideal solid lubricating films for friction reduction and anti-wear on material surfaces. However, the microtribological properties of DLC films are sensitive to many factors. In this study, DLC films were prepared through three techniques by using a self-made microwave-electron cyclotron resonance-plasma source ion implantation apparatus to determine their microtribological properties under the working conditions in a microelectromechanical system (MEMS). The three adopted techniques were unbalanced magnetron sputtering, plasma source ion implantation, and plasma-enhanced chemical vapor deposition. The diamond-like properties of the prepared films were characterized by X-ray photoelectron spectroscopy. The microtribological properties of the DLC films were analyzed by atomic force microscopy. The effects of preparation techniques, slide number, load, and relative sliding velocity on the microtribological features of the thin films were also investigated. Results reveal that in the load range of 2-20  $\mu\text{N}$ , the friction coefficients of the DLC films prepared by the three techniques are 1.8, 1.4, and 0.9 mV/nN. The prepared DLC films have lower friction coefficients than that of the Si surface (2.6 mV/nN). Under the same loading conditions, the changes of the frictional force are related to the slope of the rough peak, and the increase in frictional force is proportional to the square of the slope. The wearing depth of the DLC films is nonlinearly related to the number of wear cycles, and the wear resistance on the surface of the DLC film is worse than that in the deeper layers. Sliding velocity slightly affects the friction coefficients when the normal load is several nanonewtons. This study provides references for the application of DLC films in the surface modification of MEMS devices.

*Keywords:* Diamond-like carbon, Microtribology, Atomic force microscope

### 1. Introduction

The clearance between the friction pairs of microelectromechanical systems (MEMS) is in the nanometer level. Conventional lubricating oil may produce a large viscosity and shear force on the surface of the friction pairs, thereby greatly increasing the frictional force and friction torque between the surfaces. Therefore, traditional lubrication approaches are unsuitable for solving the friction and wear encountered during the operation of movable parts in MEMS. To solve the lubrication problems in MEMS, appropriate lubricants and lubrication techniques for microscopic working conditions must be found [1]. Solid film lubrication is recognized as an effective means to determine the friction and wear in MEMS. The physical and chemical properties of a material can be improved by coating inert films with good mechanical properties and chemical activity on the surface of MEMS devices by applying various deposition methods, as these films can confer good antiwear and lubrication effects [2]. Given their low friction coefficients, excellent wear resistance, and self-lubrication, diamond-like carbon (DLC) films are regarded as the ideal solid lubricating films for realizing friction reduction and anti-wear on material surfaces, suggesting that DLC films can be potentially applied to the surface modification of microstructures in

MEMS. For this reason, many scholars have extensively investigated the tribological behaviors of DLC films [3,4]. The microtribological properties of DLC films are sensitive to many factors, including preparation technique, slide number, load, and relative sliding velocity. Thus, the microtribological characteristics of DLC films under the working conditions in MEMS must be detected.

In this study, DLC films were prepared by three techniques. The factors affecting the tribological behaviors of DLC films were analyzed by atomic force microscopy (AFM) to predict the microtribological properties of the prepared DLC films more accurately. These results can provide references for the application of DLC films in realizing friction reduction and anti-wear in the movable parts of MEMS.

### 2. State of the art

The DLC film is an ideal film for friction reduction and anti-wear. The tribological properties of DLC films could be significantly affected by the friction conditions and the surface chemical and physical states at the contact points. Zhuo Guohai et al. [5] explored the influence of different transition layers on mechanical and tribological properties of DLC films, but they did not consider the effect of the working conditions on the tribological properties. Gong Yaoting et al. [6] utilized a friction and wear apparatus to study the friction properties of DLC films. However, the working conditions for using the friction and wear apparatus

\*E-mail address: lixin97@163.com

ISSN: 1791-2377 © 2018 Eastern Macedonia and Thrace Institute of Technology. All rights reserved.

doi:10.25103/jestr.113.21

significantly differed from those for microtribological experiments. Zheng Jinhua et al. [7] analyzed the binding strength of DLC films on different metal bases. Ball-on-disk method was used to evaluate the tribological properties of films and determine the friction coefficients, fatigue life, and wear; however, the microtribological properties of the films were not evaluated. Zeng Qunfeng et al. [8] utilized GCr15 steel balls as friction pairs to examine the tribological properties of DLC films under dry atmosphere conditions with the use of a ball-on-disk tester. However, this study did not discuss the influences of the working parameters on the tribological properties. He Tengfei et al. [9] used a ball-on-disk tester to investigate lubricating performances of films in an atmosphere environment, although they did not consider the effects of sliding velocity and roughness on the tribological properties of films. Zhan Hua et al. [10] discussed the impacts of substrate roughness on the tribological properties of Cr mixed diamond-like films, but they did not analyze the influences of sliding velocity and preparation techniques. Zhang Yan et al. [11] used DLC films prepared on Si substrate by physical vapor deposition using Cr as the transition layer to investigate the influences of the mechanical properties of the probe tip on the tribological properties. However, they did not examine the microtribological characteristics of DLC films in detail. Gachot et al. [12] indicated that incorporating different elements into DLC films may influence the tribological properties of the films. When the Si content in DLC films was lower than 5 mol%, the friction coefficient at the initial friction was large, but it decreased to a stable value over time. The maximum value of the friction coefficients decreased as the Si content increased. The structure of the DLC film is the main factor that determines its tribological properties. Nevertheless, the influences of the working conditions on the microtribological properties were not studied. According to Erdemir et al. [13], given that DLC films have a high hardness and stiffness, a low friction coefficient cannot be acquired with a low hardness and shear stress, such as in low-hardness lubricating materials, but it is the collaborative consequence of stiffness and chemical inertness. Moreover, the friction coefficient is related to the graphitization of films in the friction process. However, limited studies have explored the microtribological properties of DLC films. Liu et al. [14] posited that graphitization is the key to determine the low friction coefficient of DLC films, and that graphitization causes the micrographite layer on the surface of DLC films to transition under the constraint of low shear stress and flow back and forth.

AFM was developed by Benning et al. as an extension of scanning tunneling microscopy. AFM has significantly promoted microtribological studies. Mate et al. [15] investigated the microtribological force for the first time by using AFM. Using a tungsten probe with a 30 nm tip radius to rub graphites and mica samples, they found that a thin layer of graphite or mica adhered onto the probe surface. At this moment, the friction was due to the interaction between the layer and the samples. In addition, they also tested the stick-slip phenomenon when the probe tip was slipped over the graphite and mica surface. Since then, numerous studies [16-18] have distinguished the characteristics of microtribology from macrofriction. Nonetheless, the microtribology mechanism remains poorly understood. At present, AFM is the main approach for evaluating surface morphology and clarifying the microtribology, wear, and adhesion mechanisms [19].

These previous works have mainly focused the tribological behaviors of DLC films under a larger load. Limited studies have examined the microtribological properties of DLC films under micro- or nanonewton load by using AFM. Even fewer studies have assessed the influences of preparation technique, slide number, load, and relative sliding velocity on the microtribological properties of DLC films. In this study, DLC films were prepared by unbalanced magnetron sputtering (UMS), plasma source ion implantation (PSII), and plasma-enhanced chemical vapor deposition (PCVD) with the use of a microwave-electron cyclotron resonance-plasma source ion implantation (MW-ECR-PSII) apparatus. The diamond-like properties of the prepared films were characterized by X-ray photoelectron spectroscopy (XPS). The microtribological properties of DLC films were evaluated by AFM. Finally, the influences of preparation technique, slide number, load, and relative sliding velocity on the microtribological properties were evaluated. The findings of this study provide references for the application of DLC films in the surface modification of MEMS devices.

The remainder of this study is organized as follows. Section 3 presents the experimental apparatus, the technological parameters for the preparation of DLC films, and the principle of microtribological experiment based on AFM. Section 4 discusses the influences of preparation technique, slide number, load, and sliding velocity of a friction pair on the microtribological properties of DLC films. The microtribological law of DLC films under the working conditions in MEMS was determined. Section 5 summarizes the conclusions.

### 3. Methodology

#### 3.1 Experimental apparatus

The MW-ECR-PSII apparatus is shown in Fig.1. An  $8.75 \times 10^{-2}$  T magnetic field was generated by adjusting the coil current in the magnetic field. In this case, the microwave frequency was equal to the cyclotron frequency of the electrons. The electrons generated rotary resonance and acquired energy in the resonant cavities. The energy electrons were collided with neutral gaseous atoms/molecular to generate high-density plasmas. In addition, the magnetic fields in the two ECR cavities can be adjusted by current and direction of magnet exciting coils to form radial magnetic field or mirror field in the main vacuum chamber. The multifunctional MW-ECR-PSII apparatus, can be used to prepare films through different techniques. (1) A magnetic controlled target was added to the apparatus to accomplish magnetron sputtering technique. A radial magnetic field was employed for magnetron sputtering. Under this condition, the radial magnetic field and the magnetic field of the magnetic controlled target were superposed. Thus, the magnetic field on the magnetic controlled target surface was not closed, and a large magnetic field component perpendicular to the target surface was generated. The plasmas generated by the discharge of the magnetic controlled target were not constrained closely to the sputtering target and were carried onto the substrate surface through collision diffusion and magnetic pressure field. Thus, the ion flow density at the base was markedly increased, forming an unbalanced magnetron sputtering. The sputtering ion density and the ion energy arriving on the substrate may be changed by adjusting the sputtering bias and the substrate bias. The distance between the sputtering

target and the substrate was adjusted by changing the height of the holder. (2) The holder was connected to a high-voltage pulse power for PSII technology. (3) The holder was connected to DC bias to accomplish a PECVD process. The microwave energy was transmitted to the electrons through resonance coupling, and the electrons that acquired energy collided with neutral gas to decompose hydrocarbon gases and produce plasmas. Then, the plasmas were deposited onto the substrate.

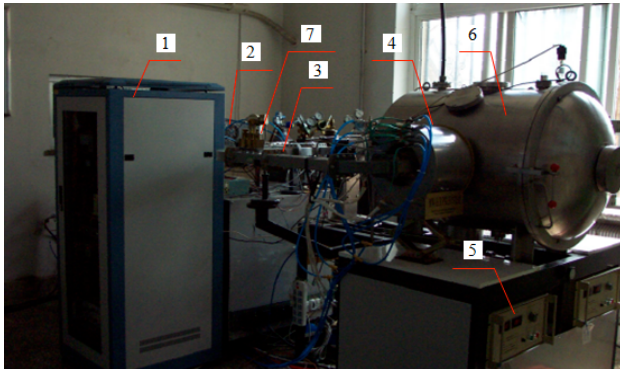


**Fig. 1.** MW-ECR-PSII apparatus  
1-control cabinet; 2- microwave source; 3-square wave guide; 4-ECR resonant cavity; 5-power supply of the ECR resonant cavity; 6-main vacuum chamber; 7-triple calibration bolt

**3.2 Preparation of DLC films**

**(1) Substrate pretreatment**

The polished Si was chosen as the substrate. The detailed technological parameters of Ar ion sputtering cleaning are listed in Table 1.

**Table. 1.** Technological parameters of sputtering cleaning

Working air pressure (Pa)	Ar flow (sccm)	Cleaning bias (V)	Cleaning time (min)
0.08	14.7	-200	10

**(2) Preparation of DLC films by UMS**

High-purity graphite was used as the carbon source (diameter=66mm), and air gas was used as the sputtering gas. The technological parameters of the DLC film preparation by UMS are shown in Table 2.

**Table. 2.** Technological parameters of UMS

Working air pressure (Pa)	Sputtering bias (V)	Deposition bias (V)	Deposition temperature (°C)	Target-substrate distance (mm)
0.09	-300	-50	300	150

**(3) Preparation of DLC films by PSII**

The holder was connected to a high-voltage pulse power supply. The technological parameters of the DLC film preparation by PSII technology are listed in Table 3.

**Table. 3.** Technological parameters of PSII

No.	Working air pressure (Pa)	CH <sub>4</sub> flow (sccm)	H <sub>2</sub> flow (sccm)	Impulse voltage (KV)
PSII-01	0.12	40	/	20
PSII-02	0.11	32.6	8.9	20
PSII-03	0.10	24.5	15.2	20
PSII-04	0.10	20.2	24	20

**(4) Preparation of DLC films by PECVD**

CH<sub>4</sub> was chosen as the carbon source. The technological parameters of the DLC film preparation by PECVD are listed in Table 4.

**Table. 4.** Technological parameters of PECVD

CH <sub>4</sub> flow (sccm)	Working air pressure (Pa)	Deposition bias voltage (V)
40	0.13	-100

**3.3 Microtribological experiment**

The principle of the microtribological experiment based on AFM is shown in Fig.2.

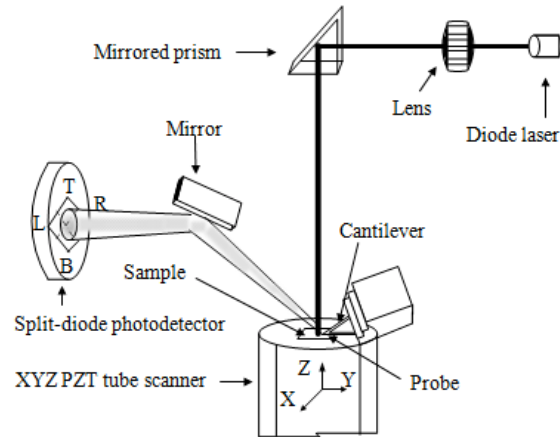


**Fig. 2.** Principle of the microtribological experiment based on AFM

Test samples were installed on a piezoelectric ceramic tube. The piezoelectric ceramic tube can scan test samples accurately along the horizontal X and Y directions and control the distance between the samples and the probe along the direction perpendicular to Z. The force-sensitive element was the V-shaped micromechanical cantilever, and the microprobe with an atomic line width was placed at the free end of the cantilever. The cantilever was tilted backward by approximately 10° relative to the horizontal plane. A laser beam emitted by a semiconductor laser was collimated to the free end of the cantilever beam. The laser beam reflected by a mirror surface onto the photodiode was used as a four-quadrant photosensitive detector. When the samples were scanned from front to back perpendicular to the cantilever, the frictional force between the samples and the probe may produce torque of cantilevers. In this way, the reflected laser beam generated an intensity difference in the quadrants L and R of the photosensitive detector, and the intensity difference can be transformed into electrical signals. Combined with deflection of the cantilever, the frictional force can be acquired. The height of the piezoelectric ceramic tube can be controlled by adjusting its voltage based on the feedback circuit, so that the normal load is maintained constant in the entire scanning process when the cantilever moves perpendicular to cantilevers. The friction coefficient was obtained by measuring the friction force under different normal loads. Fluctuations in the surface morphology caused the probe tip to move up and down in the vertical direction, which changed the direction of the reflected laser beam and the intensity at the photosensitive detectors in the T and B quadrants. Thus, the surface morphology of the samples can be measured.

4. Result analysis and discussion

4.1 Characterization of DLC films

The XPS full spectra of DLC films prepared by UMS, PSII, and PECVD are shown in Fig. 3.

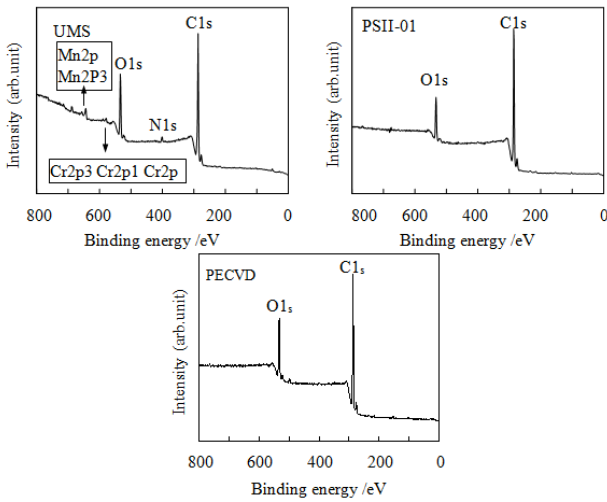


Fig. 3. XPS full spectra of the DLC films

The DLC films were primarily composed of carbon and parts of oxygen. The O1s peak was attributed to physically adsorbed oxygen on the surface. The XPS full spectrum of the DLC film prepared by UMS revealed other elements that originated from the target holder sputtered by Ar ions. The spectra were decomposed and analyzed using the Gaussian curve equation according to the spectral peak shape of the DLC samples. The binding energy spectra of the C1s electrons of three DLC films are shown in Figs. 4–6.

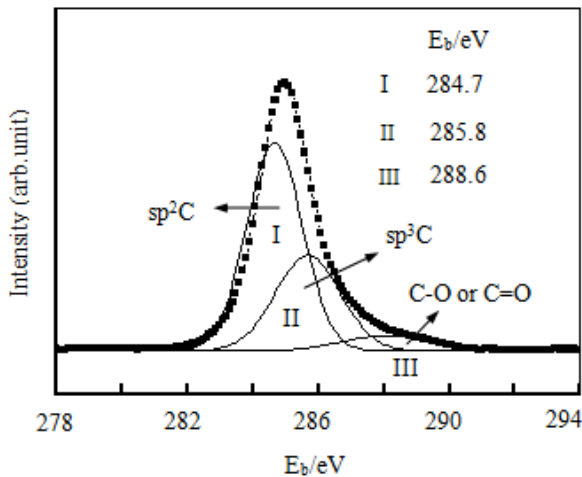


Fig. 4. Binding energy of the C 1s electrons in the DLC film prepared by UMS

The C1s spectra of the films can be divided into three peaks. The binding energy of one peak was approximately 284.5 eV, which corresponded to the binding energy of  $sp^2$  C. The binding energy of the second peak was approximately 285.5 eV, which corresponded to the binding energy of  $sp^3$  C. The binding energy of the third peak was approximately 288.0 eV, which was the binding energy of the C-O or C=O bonds. The areas of different peaks can be calculated by integral operation. The area ratio can be used to evaluate content ratio of C in different chemical binding

states in the film [20,21]. The decomposed spectra are listed in Table 5. The highest  $sp^3$ C content was displayed by the DLC film prepared by PSII-01 had (37.9%), followed by those prepared by UMS and PECVD.

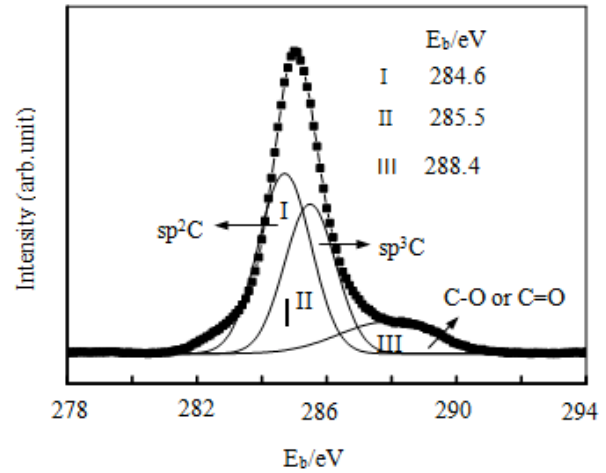


Fig. 5. Binding energy of the C1s electrons in the DLC film prepared by PSII

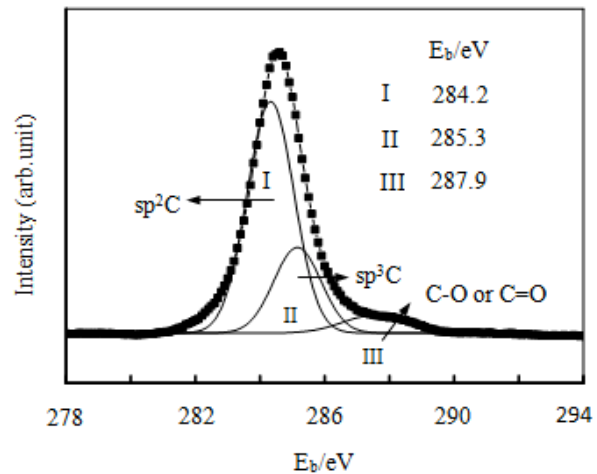


Fig. 6. Binding energy of the C1s electrons in the DLC film prepared by PECVD

Table 5. Analysis of the C 1s spectra

Preparation technology	$sp^3$ binding energy (eV)	$sp^2$ binding energy (eV)	$sp^3$ C content
MS	285.8	284.7	32.3%
PSII	285.5	284.6	37.9%
PECVD	285.3	284.2	25.4%

4.2 Microtribological properties of DLC films

The microtribological experiment was conducted on the DLC films by using the Seiko II-SPA400 AFM and triangular  $Si_3N_4$  cantilever (normal elastic coefficient: 0.09 N/m). The diameter of the probe tip was smaller than 50 nm. The experimental conditions were set as follows: room temperature, 20 °C; relative humidity, 40%–50%; transverse scanning rate, 500nm/s; and scanning range, 500nm×500 nm. In view of the complexity of the calibration for lateral force (friction force) and the absence of a uniform calibration method, the frictional force was only expressed by feedback voltage signals. In the experiment, three positions were set on each sample, and the mean frictional force of these three points was used as the experimental result. The applied

normal loads were 2, 3.8, 5.6, 7.4, 9.2, 11.0, 13.8, 15.6, 17.4, and 19.2  $\mu\text{N}$ . The friction coefficient (mV/nN) could be acquired from the relation curve between the frictional force and the load. Prior to the experiment, the surface morphology and surface adhesive force of the samples were observed and tested by AFM.

**(1) Effects of preparation technique on the frictional coefficient of the DLC films**

The relation curve between the frictional force and the load is shown in Fig. 7.

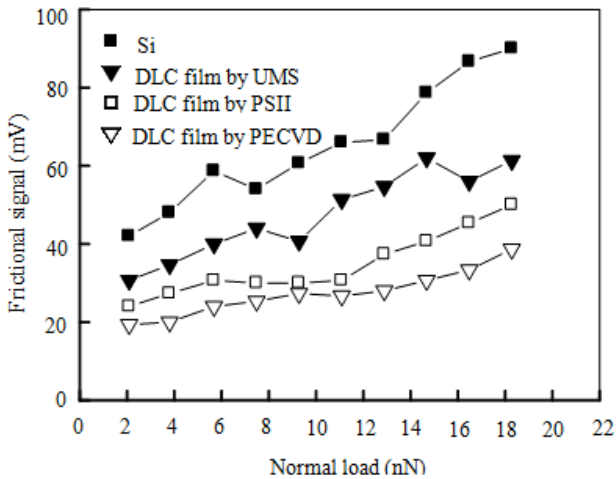


Fig. 7. Relation curve between the frictional force and the loads

In the load range of 2–20  $\mu\text{N}$ , the frictional force was linear to the loads. The frictional force signal between the DLC films and the  $\text{Si}_3\text{N}_4$  tip was smaller than the frictional force signal between the Si surface and the AFM tip. Moreover, the slope (friction coefficient) of the relation curve was smaller for the DLC films. The frictional coefficients of Si and the DLC films prepared by UMS, PSII, and PECV were 2.6, 1.8, 1.4, and 0.9 mV/nN, respectively. The DLC films had a low surface energy, and the graphite phase in the films exerted a lubrication effect [22]. Under the same load, a small frictional force appeared when the probe slid on the DLC films. The DLC films prepared by PSII and PECVD contained hydrogen, resulting in their relatively low surface energy. Moreover, hydrogen induced a lubrication effect in the microtribological process. Therefore, the DLC films prepared by PSII and PECVD had relatively smaller frictional coefficients. Among the DLC films, that prepared by PECVD had the smoothest surface; therefore, it had the minimum friction force and friction coefficient. Anisotropic friction was not observed in the microtribological experiment, because the DLC film is a non-crystalline material. Given that the contact between the AFM and the Si surface was elastic under low loads, the microbiology of the probe on the Si surface had no anisotropic friction. The frictional anisotropism was caused by the anisotropism of the monocrystal plastic deformation [23].

After the microtribological experiment was conducted on the DLC films, the used probe was further used to rub the Si surface. The worn probe tip decreased the friction coefficients, as shown in Fig. 8, suggesting that material transfer occurred during the scanning contact between the  $\text{Si}_3\text{N}_4$  tip and the DLC films. The transfer layer that formed on the  $\text{Si}_3\text{N}_4$  tip surface may modify the tip and relieve the microtribology.

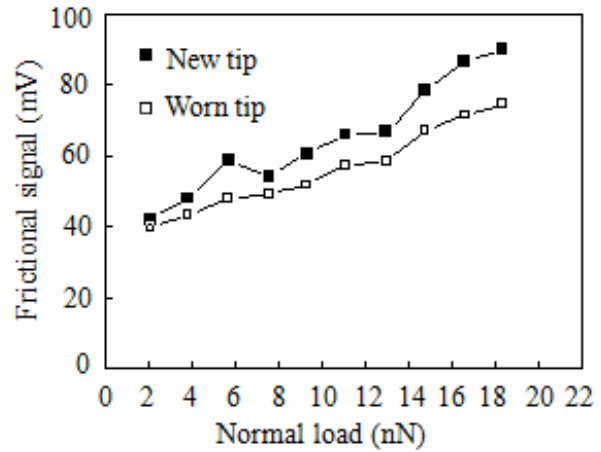


Fig. 8. Experimental comparison between the new and worn tips

**(2) Effects of adhesion on the micro frictional force of DLC films**

The experimental results were linearly fitted, and the fitted curves did not pass point (0, 0) due to the adhesion effect. Under a light normal load, the microfrictional force of the DLC film was not mainly generated by normal loads, such as macrofrictional force. However, it was sensitive to other factors, such as surface adhesive force. The adhesion phenomenon was the interaction among the molecular forces on the interface. Adhesion was the main factor that influenced the sliding friction under microloads. According to the microtribological experimental results, the relationship between the frictional force and the load can be summarized as follows:

$$F = \mu N + A \tag{1}$$

where A is a constant mainly determined by the cohesive force. The cohesive force was related to the material surface properties, ambient temperature, humidity, load, and sliding velocity in the experiment. The adhesive force on the DLC film surface ranged between 3 and 8 nN, whereas that on the Si surface was 11 nN. Therefore, A of the Si surface was relatively large. When the normal load was zero, the frictional force was completely determined by the adhesive force. In this case, the friction was reflected by the adhesive friction. The adhesive frictional mechanism is shown in Fig. 9.

Adhesive bonds developed among atoms when the probe tip came in contact with the sample surface (Fig. 9a). Under balanced conditions, the energy of the frictional system was minimum, and all atoms were at the balanced position. When the force F was applied to the probe tip, the probe tip may slightly slide (sliding distance= $\Delta x$ ) on the sample surfaces. Consequently, some old adhesive bonds were broken, and new adhesive bonds were formed (Fig. 9b).

In this process, the corresponding atoms generated forced movements, and the residual energies of these atoms were transmitted to the neighborhood atoms in vibration (heat) energies, which were called the dissipated energy. The energy can be deduced by:

$$\Delta W = \sum_k \Delta w_k \tag{2}$$

Where  $\Delta w_k$  is the increment of the energies among single atoms. Thus, the formula for the sliding frictional force can be derived as:

$$F = \Delta W / \Delta x \quad (3)$$

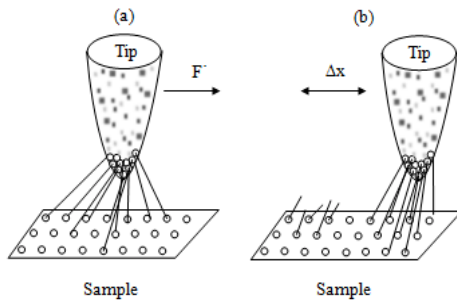


Fig. 9. Mechanism of adhesive friction

The contact region was assumed to be a plane with an area of  $A$ , and the probe tip and samples were made of the same materials. The corresponding adhesive energy was  $2\gamma A$ , where  $\gamma$  was the surface energy of the material. Upon the occurrence of small sliding, the total energy added to the friction system from the breaking of old adhesive bonds and the formation of new adhesive bonds was equal to the adhesive energy. Therefore, the following formula can be gained:

$$F = 2\gamma A / \Delta x \quad (4)$$

The effects of adhesive effect on microtribology can be determined by conducting a preliminary discussion on the mechanism of cohesive friction. The sliding process still subjected the probe tip to an amount of friction even when the applied load was negative. This feature is important in microtribology.

### (3) Effects of surface morphology on the frictional force of DLC films

The distributions of the frictional force and surface morphology of the DLC film prepared by PECVD are shown in Fig. 10.

As shown in Fig. 10, the changes in the surface morphology corresponded to the changes in the frictional force. The frictional force significantly changed with the great fluctuations of the surface morphology, and they have the same variation period. However, the peak position of the surface morphology exhibited a deflection with the peak position of the frictional force. The effects of the surface morphology on the frictional coefficients can be explained by the “racket model” of microtribology proposed by Ruan and Bhushan et al. [24]. The sliding of the probe tip over the sample surface was similar to the movement of the pawl along the racket gear edge. The slope of the rough peak was the key factor that determined the frictional coefficient. The scenario in which the probe tip is scanning the roughness peak is shown in Fig. 11. The normal load ( $W$ ) applied on the sample surface was a fixed value, assuming that the direction that was perpendicularly downward.  $F$  was the frictional force changing with the surface morphologies.  $N$  and  $S$  were the normal and tangential forces of the surface roughness peak, respectively.  $\theta$  was the angle between the roughness peak and the horizontal direction.

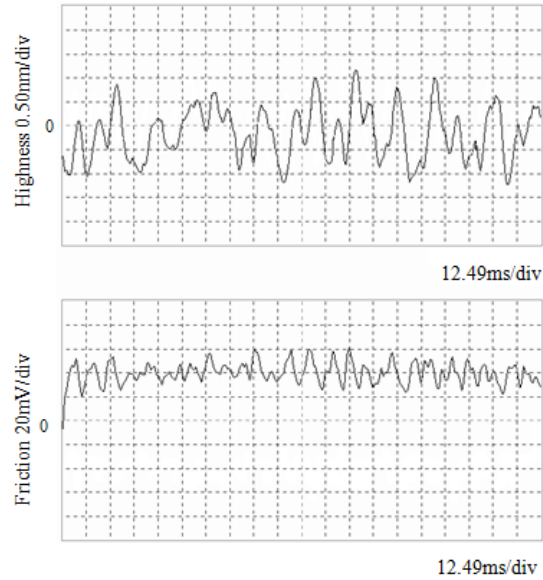


Fig. 10. Friction force and surface morphology of the DLC film prepared by PECVD

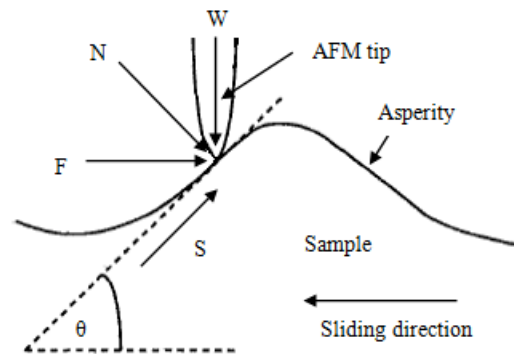


Fig.11. AFM tip scanning the roughness peak

When the probe tip increases along an inclined plane, the balance relation of the force can be reflected as:

$$N = W \cos \theta + F \sin \theta \quad (5)$$

$$S = F \cos \theta - W \sin \theta \quad (6)$$

At relative movement,  $S/N = \mu_0$ , where  $\mu_0$  is the frictional coefficient when roughness is neglected. Given the roughness (racket), the friction coefficient can be calculated as:

$$\mu_1 = F/W = (\mu_0 + \tan \theta) / (1 - \mu_0 \tan \theta) \quad (7)$$

where  $\mu_1$  is the local frictional coefficient. When  $\mu_0 \tan \theta = 1$ , Eq. (7) can be rewritten as:

$$\mu_1 \approx \mu_0 + \tan \theta \quad (8)$$

When the probe tip slides downward along the inclined plane,  $\tan \theta$  is a negative, and the local friction coefficient ( $\mu_2$ ) is:

$$\mu_2 \approx \mu_0 + \text{tg}\theta = \mu_0 - |\text{tg}\theta| \quad (9)$$

When the roughness peak is symmetric, the mean friction coefficient ( $\mu_{avg}$ ) during the scanning of the probe tip over the whole roughness peak is:

$$\mu_{avg} = (\mu_1 + \mu_2) / 2 \approx \mu_0(1 + \text{tg}^2\theta) \quad (10)$$

According to Eq. (10), if  $\mu_0 \text{tg}\theta$  is small, the symmetric roughness peak makes the growth of the microtribological coefficient proportional to  $\text{tg}^2\theta$ . The microtribological coefficient was closely related to the slope of the roughness peak. Moreover, the frictional coefficient at the surface concave or convex increased gradually. Thus, the changes in the frictional force was related to the slope of the roughness peak under the same load, and the increase was proportional to  $\text{tg}^2\theta$ .

#### (4) Effects of the sliding velocity on the frictional force

The relation curve between the sliding velocity and the frictional force (load: 10 nN) is shown in Fig. 12.

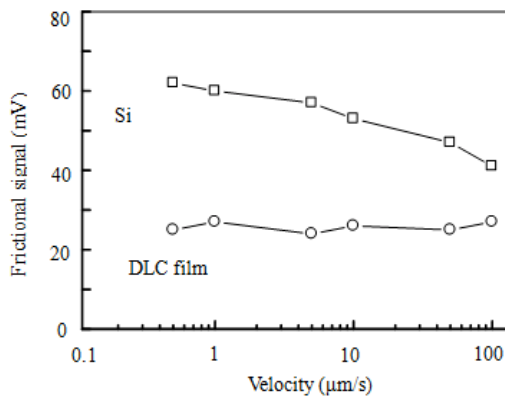


Fig. 12. Relation curve between the sliding velocity and the frictional force (load: 10 nN)

For Si, the frictional force was reduced as the sliding speed of the probe tip increased. The sliding velocity exerted an insignificant effect on the tribological properties of the DLC films, implying that that the friction mechanism of DLC films may not change with the sliding velocity.

In the case of Si, when the sliding velocity was high, no adequate time was available to form a new water half-moon surface after the breakage. In other words, the capillary force depended not only on the amount of water but also on the contact time. The production of capillaries was not an instant process. Furthermore, the tribochemical reaction was critical in this process. The high sliding velocity caused a tribochemical reaction among the water molecules, Si (naturally  $\text{SiO}_2$ ), and the  $\text{Si}_3\text{N}_4$  tip.

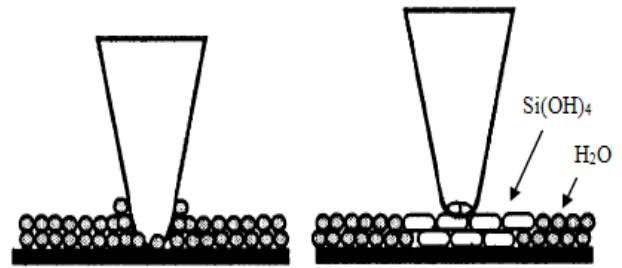
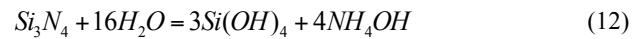


Fig.13. Tribochemical reactions

The tribochemical reactions are shown in Fig.13, and the corresponding reaction are as follows [25]:



The  $\text{Si(OH)}_4$  layer on the sliding surface had a low shear strength. The frictional force of Si decreased due to the breakage of the water half-moon surface and the formation of the  $\text{Si(OH)}_4$  layer. In view of the strong hydrophobicity, the surface of the DLC films can only absorb few water molecules from the ambient environment, resulting in the absence of the breakage of the water half-moon surface and the tribochemical reactions. Consequently, the frictional force on the DLC film surface may remain constant as the sliding velocity changed.

#### 4.3 Microwear properties of DLC films

A microwear experiment was performed on the DLC films by using AFM. The probe tip was reciprocated on the surface of the DLC films to study the microwear properties under different loads. Prior to the experiment, the surface morphologies of the samples under the normal load of 200 nN were measured to determine the standard wearing depth. Moreover, contamination or defects on sample surface may be calibrated. Second, the wear on sample surface under the chosen loads was tested. The sliding way of the diamond probe tip on the sample surface was set as follows:  $2\mu\text{m}$  along the longitudinal direction, a mini step pitch along the transverse direction, and backward by the same distance. Consequently, a  $2\mu\text{m} \times 2\mu\text{m}$  square wearing surface was scanned in the center of the sample surface. Repeated multiple wearing movements can be realized by controlling the motion of the ceramic tube. Loads and wearing times were selected based on the experimental conditions or determined by tests. In the microwear study, the wearing loss based on the weight or volume reduction of samples before and after the experiment was unsuitable due to the extremely small abrasion loss. In general, the wear resistance properties of the samples were expressed by the wearing depth or ultimate wearing times. Thus, the wear resistance capacity of the DLC films was expressed by the wearing depth. The probe scanned the square wearing region under 200nN at the end of the wear experiment. The wearing depth was measured based on the relationship between the signals and the height (Fig. 14).

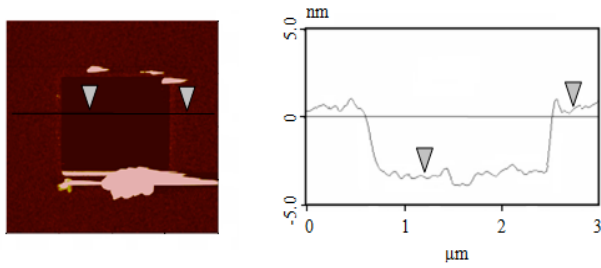


Fig. 14. Measurement of the wearing depth

**(1) Effects of preparation methods on the wear resistance of the DLC films**

The wearing losses of the samples under 22 μN load and twice wearing cycles are shown in Fig. 15.

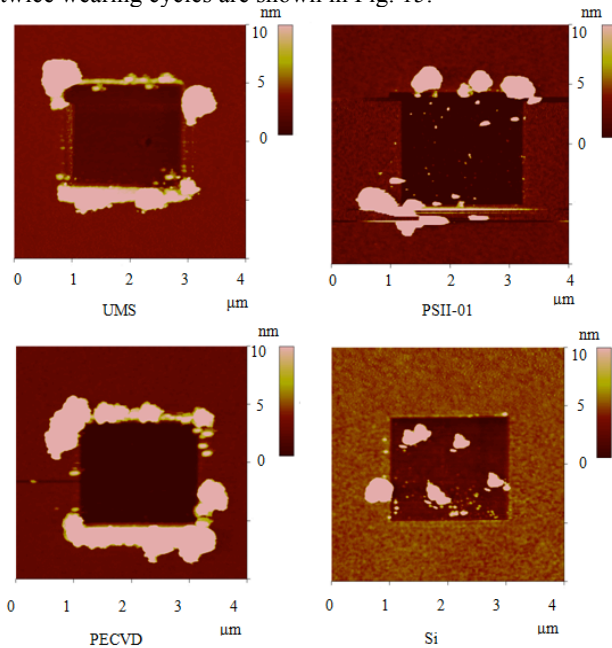


Fig. 15. Wearing mark of the samples

The experimental results are summarized in Table 6. The prepared DLC films displayed a better wear resistance capacity than that of the Si substrate. Among all DLC films, that prepared by PSII achieved the best wearing resistance capacity, followed by those prepared by PECVD and UMS. The reasons for such have been elaborated previously.

**Table 6.** Wear experimental results of DLC films

No.	Surface roughness (nm)	Wear depth (nm)	Friction coefficient
UMS	0.40	3.88	0.17
PSII-01	0.267	2.3	0.11
PECVD	0.25	3.52	0.10
Si	0.67	6.4	0.31

**(2) Effects of the number of wearing cycles on the wear resistance**

The relation curves of the wearing depth and the number of wearing cycles for the prepared DLC films are shown in Fig. 16.

The wear depth of the film increased as the number of wear cycles increased. The wear depth of silicon was approximately linear with the number of cycles, whereas the wear depth of the DLC films was nonlinear with the number of cycles. Thus, the wear resistance capacity of the surface of the DLC films might be significantly inferior to that of

the deep layers. A soft film was formed on the surface of the DLC films [13] (graphite structure). This soft film was conducive for reducing the frictional coefficient but was disadvantageous for the wear resistance capacity. Given the existence of this soft film, the wearing depth on the DLC films increased sharply at an early stage, whereas the wear resistance capacity of the DLC films was markedly improved after the surface layer was worn, thereby gradually stabilizing the wearing depth. The DLC film prepared by PECVD contained high H and C–H bonds on the surface, resulting in the deteriorating wear resistance capacity. Thus, the wear resistance capacity of the DLC film prepared by PECVD was inferior to that of the DLC film prepared by PSII. The DLC film prepared by UMS was similar to that prepared by PECVD. As the number of wearing cycles was increased, the wear resistance capacities of all three DLC films were increased significantly.

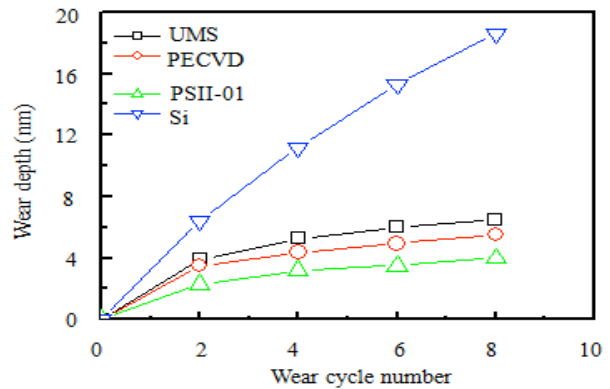


Fig. 16. Relation curves between the wearing depth and the number of wearing cycles

**(3) Effects of the air source in PSII on the wear resistance of DLC films**

The effects of H<sub>2</sub> flow ratio on the microtribological properties of the DLC film prepared by PSII are shown in Table 7. As the H<sub>2</sub> flow ratio increased, the wearing depth on the DLC film initially rapidly decreased and subsequently slightly increased. Given that the diamond-like components in the film increased as the H<sub>2</sub> flow ratio increased, the wear resistance capacity of the DLC film was improved. However, the surface roughness increased as the H<sub>2</sub> flow ratio increased, deteriorating the wearing resistance capacity. These findings suggest that the sp<sup>3</sup> bond content and the surface roughness can significantly influence the wearing resistance capacity of DLC films.

**Table 7.** Effects of hydrogen flow ratio on the wear behavior of the DLC films

Samples	CH <sub>4</sub>	H <sub>2</sub>	Surface roughness (nm)	wearing depth (nm)
PSII-01	40	0	0.267	2.30
PSII-02	32.6	8.9	0.374	1.28
PSII-03	24.5	15.2	0.507	1.55
PSII-04	20.2	24	0.572	1.93

**5. Conclusions**

In this study, DLC films were prepared by UMS, PSII, and PECVD. The microtribological properties of DLC films

under the working conditions in MEMS were investigated by AFM. The influences of preparation technique, sliding number, load, and relative sliding velocity on the microtribological properties of DLC films were discussed. The following conclusions could be drawn:

- (1)The DLC films prepared by PSII and PECVD had a relatively low surface energy due to the hydrogen content. Hydrogen presented a lubricating effect during the microtribological process. These two films had relatively small friction coefficients.
- (2)Material transfer occurred during the scanning contact between the AFM tip and the DLC films, resulting in the formation of a transfer layer on the surface of the AFM tip. This transfer layer can modify the AFM tip, thereby relieving microtribology.
- (3)Adhesive effect can significantly influence the microtribology significantly. A frictional force was still present when the applied load was negative. Under the same loads, the changes in the frictional force were related to the slope of the roughness peak, and the increase in frictional force was proportional to the square of the slope.

(4)A nonlinear relationship existed between the wear depth on the DLC films and the number of wear cycles, indicating that the wear resistance on the surface of the DLC film was worse than that in the deeper layers.

The working conditions in MEMS devices were simulated by AFM, and a new understanding on the microtribological law of DLC films was proposed. The results of this study provide references for the application of DLC films in the surface modification of MEMS devices. Given that the real working conditions in MEMS devices are more complex, DLC films prepared on the surface of movable parts were employed to study their microtribological properties, and other influencing factors should be considered in future studies.

#### Acknowledgements

This work was supported by the National Natural Science Foundation of China (Grant No. 50135040).

This is an Open Access article distributed under the terms of the Creative Commons Attribution License



#### References

1. Polaki, S. R., Kumar, N., Madapu, K., "Interpretation of friction and wear in DLC film: role of surface chemistry and test environment". *Journal of Physics D Applied Physics*, 49(44), 2016, pp.445302-445316.
2. Wang, J., Zhang, K., Wang, F., Zheng, W., "Improving frictional properties of DLC films by surface energy manipulation". *RSC Advances*, 8(21), 2018, pp. 11388-11394.
3. Manimunda, P., Alazizi, A., Kim, S. H., "Shear-induced structural changes and origin of ultralow friction of hydrogenated diamond-like carbon (DLC) in dry environment". *ACS Applied Materials & Interfaces*, 9(19), 2017, pp.16704-16714.
4. Arslan, A., Masjuki, H. H., Varnan, M., Kalam, M. A., "Effect of change in temperature on the tribological performance of micro surface textured DLC coating". *Journal of Materials Research*, 31, 2016, pp.1837-1847.
5. Zhuo, G. H., Ke, P. L., Li, X. W., Wang A. Y., Zhao, Y. C., "Influence of different interlayers on mechanical and tribological properties of DLC films". *China Surface Engineering*, 28(6), 2015, pp.39-46.
6. Gong, Y. T., Peng, X., "Anti-oxidation and tribology properties of MPCVD DLC films". *Surface Technology*, 47(2), 2018, pp.136-143.
7. Zheng, J. H., Li, C. H., Zhang, C., Chao, Y. F., "Friction properties of DLC film on different metal substrates". *Optics and Precision Engineering*, 21(6), 2003, pp.1544-1552.
8. Zeng, Q. F., Yu, F., Dong, G. N., Mao, J. H., Lin, K. S., "Growth and tribological property characterization of diamond-like-carbon films". *Chinese Journal of Vacuum Science and Technology*, 33(4), 2013, pp. 378-381.
9. He, T. F., Wu, Y. Z., Xu, J., "Structure and tribological properties of MoS<sub>2</sub>/DLC multilayer films with different modulation periods". *Tribology*, 37(1), 2017, pp.35-42.
10. Zhan, H., Wang, R. J., Li, Z. D., "Effects of film fragments on wear properties for W-DLC films under boundary lubrication conditions". *China Surface Engineering*, 31(2), 2018, pp. 59-65.
11. Zhang, Y., Dong, M., Li, M., "Nano-tribological properties of diamond-like carbon films". *Tribology*, 35(2), 2015, pp. 241-247.
12. Gachot, C., Rosenkranz, A., "A critical assessment of surface texturing for friction and wear improvement". *Wear*, s372-373, 2017, pp.21-41.
13. Erdemir, A., Bindal, C., Fenske G. R., "Characterization of transfer layers forming on surfaces sliding against diamond-like carbon". *Surface and Coating Technology*, s86-87(1), 1996, pp.692-697.
14. Liu, Y., Erdemir, A., Meletis, E. I., "Influence of environmental parameters on the frictional behavior of DLC coatings". *Surface and Coating Technology*, s94-95(545), 1997, pp.463-468.
15. Mate, C. M., McClelland, G. M., Erlandsson, R., "Atomic scale friction of a tungsten tip on a graphite surface". *Physics Review Letters*, 59(17), 1987, pp.1942-1945.
16. Arslan, A., Masjuki, H. H., "Effects of texture diameter and depth on the tribological performance of DLC coating under lubricated sliding condition". *Applied Surface Science*, 356, 2015, pp.1135-1149.
17. Chen, Y. N., Ma, T. B., Chen, Z., "Combined effects of structural transformation and hydrogen passivation on the frictional behaviors of hydrogenated amorphous carbon films". *Journal of Physical Chemistry C*, 119(28), 2015, pp.16148-16155.
18. Lotfi, R., Jonayat, A., Hempstead, R., "A reactive force field study on the interaction of lubricant with diamond-like carbon structures". *Journal of Physical Chemistry C*, 120(48), 2016, pp.27443-27451.
19. Wang, C., Li, B., Ling, X., "Super lubricity of hydrogenated carbon films in a nitrogen gas environment: adsorption and electronic interactions at the sliding interface". *RSC Advances*, 7(1-5), 2017, pp.3025-3034.
20. Susumu, T., Radek, J., Masanori, S., "Chemical structural analysis of diamond like carbon films: I. surface growth model". *Surface Science*, 668, 2018, pp.29-35.
21. Takabayashi, S., Yang, M., Eto, T., "Controlled oxygen-doped diamond-like carbon film synthesized by photoemission-assisted plasma". *Diamond and Related Materials*, 53, 2015, pp.11-17.
22. Gao, G. T., Mikulski, P. T., Harrison, J. A., "Molecular-scale tribology of amorphous carbon coatings: effects of film thickness, adhesion, and long-range interactions". *Journal of the American Chemical Society*, 124(24), 2002, pp.7202-7209.
23. Gatzert, H. H., Beck, M., "Investigations on the friction force anisotropy of the silicon lattice". *Wear*, 254(11), 2003, pp.1122-1126.
24. Ruan, J.A., Bhushan, B., "Atomic-scale and microscale friction studies of graphite and diamond using friction force microscopy". *Journal of Applied Physics*, 76(9), 1994, pp.5022-5035.
25. Liu, H., Bhushan, B., "Nanotribological characterization of molecularly thick lubricant films for applications to MEMS/NEMS by AFM". *Ultramicroscopy*, 97(1), 2003, pp.321-340.